Heliyon 9 (2023) e16522

Contents lists available at ScienceDirect

Heliyon

journal homepage: www.cell.com/heliyon

Research article

Analysis of blood flow of unsteady Carreau-Yasuda nanofluid with viscous dissipation and chemical reaction under variable magnetic field

Mubashir Qayyum [a], Muhammad Bilal Riaz [b,c,d,*], Sidra Afzal [a]

[a] *Department of Sciences and Humanities, National University of Computer and Emerging Sciences, Lahore, Pakistan*
[b] *Faculty of Technical Physics, Information Technology and Applied Mathematics, Lodz University of Technology, 90-924 Lodz, Poland*
[c] *Department of Computer Science and Mathematics, Lebanese American University, Byblos, Lebanon*
[d] *Department of Mathematics, University of Management and Technology, 54770 Lahore, Pakistan*

A R T I C L E I N F O

Keywords:
Unsteady flow
Blood flow
Carreau-Yasuda fluid model
Magnetohydrodynamic
Thermophoresis
Brownian motion
Porous medium
Activation energy
Viscous dissipation

A B S T R A C T

Blood flow analysis through arterial walls depicts unsteady non-Newtonian fluid flow behavior. Arterial walls are impacted by various chemical reactions and magnetohydrodynamic effects during treatment of malign and tumors, cancers, drug targeting and endoscopy. In this regard, current manuscript focuses on modeling and analysis of unsteady non-Newtonian Carreau-Yasuda fluid with chemical reaction, Brownian motion and thermophoresis under variable magnetic field. The main objective is to simulate the effect of different fluid parameters, especially variable magnetic field, chemical reaction and viscous dissipation on the blood flow to help medical practitioners in predicting the changes in blood to make diagnosis and treatment more efficient. Suitable similarity transformations are used for the conversion of partial differential equations into a coupled system of ordinary differential equations. Homotopy analysis method is used to solve the system and convergent results are drawn. Effect of different dimensionless parameters on the velocity, temperature and concentration profiles of blood flow are analyzed in shear thinning and thickening cases graphically. Analysis reveals that chemical reaction increases blood concentration which enhance the drug transportation. It is also observed that magnetic field elevates the blood flow in shear thinning and thickening scenarios. Furthermore, Brownian motion and thermophoresis increases temperature profile.

1. Introduction

Study of non-Newtonian fluid models is very important for understanding the blood flow in human body. It became very interesting to model and simulate blood flow problems and incooperate the observed effects in human body as a result of such problems. Stretching arteries under high blood pressure, hypertension, or other physiological traumas are much important to be analyzed under varying conditions. Heart pumps blood in cycles, pumping blood in and out periodically, known as systole and diastole. In humans, unsteady nature of blood flow is causing deaths at high rate in cardiovascular disease patients throughout the world. In this regard various phenomena have been observed by many researchers. Few of the related studies can be found in [1–5]. Carreau-Yasuda

* Corresponding author.
E-mail address: muhammad.riaz@p.lodz.pl (M.B. Riaz).

https://doi.org/10.1016/j.heliyon.2023.e16522
Received 18 November 2022; Received in revised form 17 May 2023; Accepted 18 May 2023

Available online 24 May 2023

Nomenclature

Parameters with units

x, y	axial coordinates	m
t	temporal coordinate	s
$\mathbb{V}$	velocity	$\mathrm{m\,s^{-1}}$
u, v	velocity along x and y axis	$\mathrm{m\,s^{-1}}$
ξ	time constant	
k^*	porosity rate	$\mathrm{m^2}$
ν	kinematic viscosity ($\mathrm{m^2\,s^{-1}}$)	s
σ^*	electric conductivity	$\mathrm{Sm^{-1}}$
k	thermal conductivity	W/m K
B_0	magnetic field strength	$\mathrm{A\,m^{-1}}$
T, C	temperature and concentration	K, $\mathrm{kg\,m^{-3}}$
ρ	density	$\mathrm{kg\,m^{-3}}$
(ρC_p)	specific heat	J/kg K
τ	extra stress tensor	$\mathrm{kg\,m^{-1}\,s^2}$
D_T	thermophoresis diffusion coefficient	$\mathrm{kg\,m^{-1}\,s^{-1}\,K^{-1}}$
k_0	Boltzmann constant	$\mathrm{W\,m^{-2}\,K^{-4}}$
μ_0	dynamic viscosity	$\mathrm{kg\,m^{-1}\,s^{-1}}$
k_r^2	chemical reaction rate	$\mathrm{M\,s^{-1}}$
E_a	activation energy	$\mathrm{J\,M^{-1}}$
D_B	Brownian diffusion coefficient	$\mathrm{kg\,m^{-1}\,s^{-1}}$
a, c	positive constants	$\mathrm{s^{-1}}$

Dimensionless parameters

$F(\eta)$	non-dimensional velocity
$\theta(\eta)$	non-dimensional temperature
$\phi(\eta)$	non-dimensional concentration
η	independent variable
S	mass transfer parameter
A	stretching ratio
Pr	Prandtl number
We	Weissenberg number
β	porosity parameter
M	Hartman number
Ec	Eckert number
$\tilde{A}$	unsteadiness parameter
Nt	thermophoresis parameter
σ	reaction rate parameter
Sc	Schmidt number
Nb	Brownian motion parameter
δ	relative temperature ratio
ν^*	activation energy parameter
$\hbar$	convergence control parameter

nanofluid modeled in this manuscript depicts the non-Newtonian blood flow behavior in both shear thinning and thickening cases. Similarly Boyd et al. [6] utilized Boltzmann lattice method to analyze Carreau-Yasuda blood flow model. Shamekhi and Sadeghy [7] studied Carreau-Yasuda model using PIM mesh free method. Andrade et al. [8] presented the turbulent flow behavior of Carreau-Yasuda fluid passing through pipes.

Magnetic field plays a vital role when treating maligns and cancer [9], tumors [10], drug targeting [11], cell separation [12], magnetic endoscopy [13] and adjusting blood flow during surgery [14]. Behavior of blood flow and temperature is essential to be studied in more controlled environment during such processes. Parkash et al. [15] studied MHD effects on bifurcated arteries. Periodic body acceleration under MHD blood flow is investigated by Das and Saha [16]. Rao et al. [17] utilized a spectral relaxation scheme to analyze a nanofluid impacted by magnetic effects flowing on an exponentially stretched surface. Recently, Tanveer et al. [18] analyzed peristaltic activity on MHD blood flow. MHD blood flow with Hall effects and Joule heating was taken into account by Bhatti and Rashidi [19]. Ramana et al. [20] investigated the MHD flow of an Oldroyd-B fluid with Cattaneo-Christov heat flux passing over a non linearly stretched sheet. Various fluid models under applied magnetic field are analyzed in literature [21–24].

Chemical reaction and activation energy are significant processes in blood flow analysis. Due to intake of different drugs in any medical treatment, chemical reactions in human blood occur more than the usual situations. Recently, various non-Newtonian fluids models are designed with the effect of chemical reaction and activation energy. Saleem et al. [25] worked on thermal analysis of radiated blood flow with buoyancy forces undergoing chemical reactions. Gangadhar et al. [26] analyzed the phenomena of non-linear thermal radiation by incorporating chemical reaction in Casson-Maxwell nanofluid flow between static disks. Ramzan et al. [27] studied flow of nanofluid with autocatalytic chemical reaction with slip conditions. Chemical reactions on Sisko fluid were considered by McCash et al. [28]. Yu et al. [29] analyzed chemically reactive flow of Ostwald-de-Waele nanofluid on a rotating disk. Khan et al. studied Walter-B fluid under activation energy and chemical reaction in [30]. Recent developments on various fluids models have also been done with such effects in [31–36].

Viscous dissipation is an irreversible process in which heat dissipates due to shear forces among adjacent fluid layers. Most recent work on blood flow with viscous dissipation is done by Gandhi et al. in [37]. They investigated blood flow with drug delivery under the effects of Joule heating and viscous dissipation. Casson nanofluid on a shrinking surface with viscous dissipation was examined by Yang et al. [38]. Megahed and Reddy introduced numerical treatment to viscoelastic fluid with viscous dissipation [39]. Chu et al. [40] did stability analysis with dual solutions on viscous dissipative cross flows under impact of magnetic field. Investigation on nanoconfined behavior of water flow from the perspective of viscous dissipation was done by Wang et al. [41]. Mabood and Mastroberardino [42] examined nanofluid flow over a stretching sheet with second order slip and viscous dissipation. Hashmi et al. [43] studied Oldroyd-B fluid with viscous dissipative flow and binary reaction over a stretching sheet.

Blood flow being periodic in normal circumstances can be modeled under periodic conditions. However, in diseased cases or accidental scenarios, unsteady blood flows are encountered. Khan et al. [44] analyzed steady Carreau fluid with activation energy in

Table 1
Comparison of present work with existing work in literature.

	Unsteady flow	Thin./thick.	Stretch.	Suc./Inj.	Visc. dissip.	Chem. Reac.	Thermo. & Brown.	Porous media
Salahuddin et al. [50]	No	No	Yes	No	No	No	No	No
Khan et al. [51]	No	No	No	No	Yes	Yes	No	No
Nazir et al. [52]	No	No	No	No	Yes	No	No	Yes
Present Work	Yes	Yes	Yes	Yes	Yes	Yes	Yes	Yes

porous medium. In light of literature elaborated above, unsteady blood flow analysis in stretching arteries under viscous dissipation, chemical reaction, Brownian motion and thermophoresis is yet to be investigated for both thinning and thickening of blood. Moreover, Table 1 is presented to signify the novelty of present study. Current investigation is motivated under unsteady environment related to the non-periodic blood flow analysis through arterial walls. After involving the aforementioned phenomenon in governing equations of fluid mechanics, mathematical model for current study is devised. Many analytical and semi-analytical approaches are utilized in literature for solution purpose of such flow problems [45–49]. For simulation purpose in this study, homotopy analysis method will be used to obtain a convergent series form solution. This scheme provides freedom of choosing the linear operator and initial guess which depicts great flexibility in how the solution is explicitly obtained. Although, this method efficiently provides series form approximate results for highly non-linear coupled differential equations but in case of various problems containing transcendental non-linearity, this method may not provide convergent results. In rest of the manuscript mathematical modeling is given in section 2, solution technique is given in section 3, results and discussion is in section 4 while conclusion is given in section 5.

2. Mathematical modeling

2.1. Flow regime

Consider the two-dimensional unsteady blood flow between two walls with distance $h(t)$ apart having time-dependent stretching in x-direction. Temperature and concentration at $y=0$ surface is time-variant denoted by $\tilde{\mathbb{T}}$ and $\tilde{\mathbb{C}}$, respectively while on the other wall at $y=h(t)$ the constant temperature and concentration are maintained as T_2 and C_2, respectively. Time-dependent magnetic field $B(t)$ acts perpendicularly along y-direction. In this study, electron-ion frequency is assumed to be small due to which induced magnetic field and Hall effects are neglected as done in [53]. Thermophoresis and Brownian motion takes place due to nanoparticle movement within Carreau-Yasuda nanofluid. Viscous dissipation and chemical reaction effects also impact the blood flow. Carreau-Yasuda fluid is treated as blood in this study, due to its similar properties exhibiting shear thinning and thickening behavior.

2.2. Carreau-Yasuda model

The extra stress tensor in modeling Carreau-Yasuda flow problem is

$$\tau=\mu_\infty+\left(\mu_0-\mu_\infty\right)\left(1+(\xi\dot{\gamma})^d\right)^{\frac{n-1}{d}}\breve{\mathbf{A}}, \tag{1}$$

where

$$\breve{\mathbf{A}}=\frac{1}{2}\left[(grad V)+(grad V)^T\right], \tag{2}$$

$$\dot{\gamma}=\sqrt{\frac{tr\left(\breve{\mathbf{A}}\right)}{2}}, \tag{3}$$

here μ_0 and μ_∞ represent the zero and infinite viscosity shear stress rates in Eq. (1) and d, n and ξ are the Carreau-Yasuda fluid parameters. $\breve{\mathbf{A}}$ and γ are the first Rivlin Erickson tensor and the shear rate respectively in Eqs. (2) and (3). Shear thinning and thickening behaviors of fluid are observed when $n<1$ and $n>1$, respectively. If $n=1$ or $\xi=0$, then fluid shows Newtonian behavior and for $d=2$ the fluid is said to be Carreau fluid. We will restrict our investigation to non-Newtonian behavior of blood which is very important in case of low shear rates and small arteries.

Let $\mu_\infty=0$, then stress tensor in Eq. (1) becomes

$$\tau=\mu_0\left(1+(\xi\dot{\gamma})^d\right)^{\frac{n-1}{d}}\breve{\mathbf{A}},$$

2.3. Problem formulation

Continuity, momentum, energy and concentration equations that govern the flow problem, are given below

$$\nabla.\mathbb{V}=0, \tag{4}$$

$$\frac{\partial u}{\partial t}=\nu\frac{\partial^2 u}{\partial y^2}-\upsilon\frac{\partial u}{\partial y}+(u_2-u)\frac{\nu}{k^*}-u\frac{\partial u}{\partial x}+u_2\frac{\partial u_2}{\partial x}+\xi^d\nu\left(\frac{n-1}{d}\right)(d+1)\frac{\partial^2 u}{\partial y^2}\left(\frac{\partial u}{\partial y}\right)^d+\frac{\sigma^*}{\rho}B^2(t)(u_2-u), \tag{5}$$

$$\frac{\partial T}{\partial t}+u\frac{\partial T}{\partial x}+\upsilon\frac{\partial T}{\partial y}=\frac{k}{(\rho c_p)}\frac{\partial^2 T}{\partial y^2}+\tau\left(\frac{D_T}{T_2}\left(\frac{\partial T}{\partial y}\right)^2+D_B\frac{\partial T}{\partial y}\frac{\partial C}{\partial y}\right)+\frac{\mu_0}{(\rho c_p)}\left(\frac{\partial u}{\partial y}\right)^2+\frac{\mu_0}{(\rho c_p)}\left(\frac{n-1}{d}\right)\xi^d\left(\frac{\partial u}{\partial y}\right)^2\left(\frac{\partial u}{\partial y}\right)^d, \tag{6}$$

$$\frac{\partial C}{\partial t}+u\frac{\partial C}{\partial x}+\upsilon\frac{\partial C}{\partial y}=D_B\frac{\partial^2 C}{\partial y^2}+\frac{\partial^2 T}{\partial y^2}\left(\frac{D_T}{T_2}\right)-k_r^2(C-C_2)\left(\frac{T}{T_2}\right)^m e^{\frac{-Ea}{k_0 T}}, \tag{7}$$

subject to following boundary conditions

$$\begin{aligned} &u=\tilde{\mathbb{U}}(x,t),\ \upsilon=\tilde{\mathbb{V}}(x,t),\ T=\tilde{\mathbb{T}}(x,t),\ C=\tilde{\mathbb{C}}(x,t)\quad at\quad y=0\\ &u=u_2(x,t)=\frac{a_2x}{1-ct},\ T=T_2, C=C_2\quad at\quad y=h(t). \end{aligned} \tag{8}$$

The unsteady parameters are as follows

$$\begin{aligned} &\Upsilon=1-ct,\ \tilde{\mathbb{U}}(x,t)=\frac{ax}{\Upsilon},\ h(t)=\sqrt{\frac{\nu\Upsilon}{a}},\tilde{\mathbb{V}}(x,t)=\frac{-V_0}{\Upsilon^{\frac{1}{2}}},\\ &\tilde{\mathbb{T}}(x,t)=T_2+\frac{T_0U_wx}{\upsilon\Upsilon^{\frac{1}{2}}},\ \tilde{\mathbb{C}}(x,t)=C_2+\frac{C_0U_wx}{\upsilon\Upsilon^{\frac{1}{2}}},\ B(t)=\frac{B_0}{\Upsilon^{\frac{1}{2}}} \end{aligned} \tag{9}$$

Similarity transformations are introduced as follows

$$\begin{aligned} &c\Psi=\sqrt{\nu x\tilde{\mathbb{U}}}F(\eta),\quad \eta=y\sqrt{\frac{\tilde{\mathbb{U}}}{\nu x}},\\ &\theta(\eta)=\frac{T-T_2}{\tilde{\mathbb{T}}-T_2},\ \phi=\frac{C-C_2}{\tilde{\mathbb{C}}-C_2}, \end{aligned} \tag{10}$$

from Ψ we can directly get $u=\frac{\partial\Psi}{\partial y}$ and $\upsilon=-\frac{\partial\Psi}{\partial x}$. After using Eqs. (9) and (10) in Eqs. (4)-(8), the system of dimensional PDEs are transformed into system of dimensionless ODEs presented in Eqs. (11)-(13) along with boundary conditions in Eq. (14).

$$F'''\left[1+(F'')^d(We)^d\left(\frac{(n-1)(d+1)}{d}\right)\right]+(M^2+\beta)(A-1)F'+FF''+A^2-F'(F'+A)+\frac{A}{2}\eta F''=0, \tag{11}$$

$$\frac{1}{Pr}\theta''+\theta'(Nt\theta'+Nb\phi')+\left(d+(n-1)(We)^d(F'')^d\right)\frac{Ec}{d}F''^2-\theta\tilde{A}\left(\frac{2}{\tilde{A}}+\frac{3}{2}+\eta\frac{\theta'}{\theta}\right)-\theta'F=0, \tag{12}$$

$$\phi''+\frac{Nt}{Nb}\theta''-Sc\sigma\phi(1+\delta\theta)^m e^{\left(\frac{-\nu*}{1+\delta\theta}\right)}-\frac{1}{2}Sc\tilde{A}(3\phi+\eta\phi')-2Sc(F'\phi-F\phi')=0, \tag{13}$$

with following dimensionless boundary conditions

$$\begin{aligned} &F(\eta)=S,\ F'(\eta)=1,\ \theta(\eta)=1,\ \phi(\eta)=1\quad \text{at } \eta=0\\ &F'(\eta)=A,\ \theta(\eta)=0,\ \phi(\eta)=0\quad \text{at } \eta=1 \end{aligned} \tag{14}$$

The dimensionless variables are

$$\begin{aligned} &We=\xi\sqrt{\frac{a^3x^2}{(1-ct)^3\nu}},A=\frac{a_2}{a},\tilde{A}=\frac{c}{a},\ \beta=\frac{\nu(1-ct)}{k^*a},\\ &M=\sqrt{\frac{\sigma^*}{\rho a}}B_0,\ Ec=\frac{(ax)^2}{c_p(T_w-T_2)(1-ct)^2},\ \Pr=\frac{(\rho c_p)\nu}{k},\\ &Nt=\frac{\tau D_T(T_w-T_2)}{\nu T_2},Nb=\frac{\tau D_B(C_w-C_2)}{\nu},\ Sc=\frac{\nu}{D_B},\\ &\sigma=\frac{k_r^2(1-ct)}{a},\ \delta=\frac{\tilde{\mathbb{T}}-T_2}{T_2},\ \nu^*=\frac{Ea}{k_0T_2},\ S=\frac{\upsilon_0}{\sqrt{a\nu}}. \end{aligned}$$

3. Solution methodology

In order to solve the modeled problem, well known homotopy analysis method is utilized in this section. The deformation equations of zeroth order and mth-order are given below.

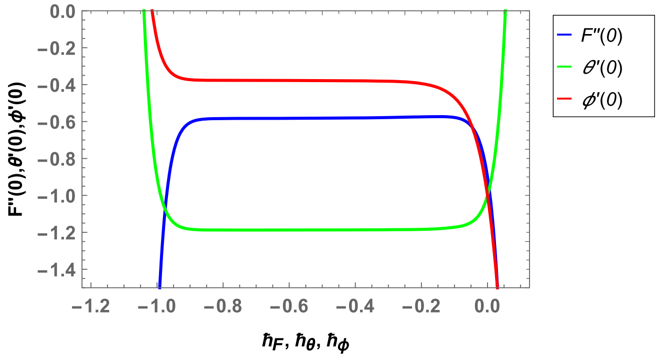

Fig. 1. Combined $\hbar$-plots.

3.1. Deformation of zeroth order

At zeroth order of deformation, the governing equations take following form

$$(1-\mathring{q})\mathcal{L}_{\zeta_j}\left[\zeta_j(\eta,\mathring{q})-\zeta_{j_{int}}(\eta)\right]=\mathring{q}\hbar_j N_{\zeta_j}\left[\zeta_j(\eta,\mathring{q})\right],$$

where $\mathcal{L}_{\zeta_j}$ are the linear operators and $j=1,2,3$ corresponds to homotopy equation of F, θ and ϕ respectively, similarly N_{ζ_j} are the nonlinear operators, $\mathring{q}$ the embedding parameter, $\zeta_{j_{int}}(\eta)$ are the initial guesses, η is the auxiliary parameter, $\zeta_j(\eta,\mathring{q})$ are the unknown function of η and $\mathring{q}$.

When we take $\mathring{q}=0$ we obtain initial approximations whereas $\mathring{q}=1$ gives us the final solutions, which are

$$\zeta_j(\eta,0)=\zeta_{j_{int}}(\eta)\ \ and\ \ \zeta_j(\eta,1)=\zeta_j(\eta),$$

3.2. mth-order deformation

For mth-order deformation, we differentiate Eqs. (11)-(13) relative to $\mathring{q}$. After putting $\mathring{q}=0$ and dividing the expressions with $m!$, we obtain

$$\mathcal{L}_{\zeta_j}\left[\zeta_{jm}(\eta)-\mathbb{X}_m\zeta_{j(m-1)}(\eta)\right]=\hbar\bar{R}_{\zeta_{jm}}(\eta),$$

here we define

$$\mathbb{X}_m=\begin{cases}0 & m\le 1,\\ 1 & \text{otherwise,}\end{cases}$$

and

$$R_{\zeta_{jm}}(\eta)=\frac{1}{(m-1)!}\left.\frac{\partial^m\check{N}_{\zeta_j}\left[\zeta_j(\eta,\mathring{q})\right]}{\partial\mathring{q}^m}\right|_{\mathring{q}=0}$$

The linear operators at j and corresponding initial guess are chosen as

$$\left.\begin{array}{llll}\text{At } j=1, & \mathcal{L}_{\zeta_1}=F''', & \zeta_{1_{int}}=\zeta_{F_{int}}=S+\eta+\frac{(A-1)}{2}\eta^2,\\ \text{At } j=2, & \mathcal{L}_{\zeta_2}=\theta'', & \zeta_{2_{int}}=\zeta_{\theta_{int}}=1-\eta,\\ \text{At } j=3 & \mathcal{L}_{\zeta_3}=\phi'', & \zeta_{3_{int}}=\zeta_{\phi_{int}}=1-\eta,\end{array}\right\}$$

3.3. Convergence analysis

In this section, convergence of series solution for velocity, temperature and concentration profile is determined. In Fig. 1 the $\hbar$-curves for 24^{th} iteration of auxiliary variables have been plotted. Region of convergence for velocity, temperature and concentration profile are $-0.89\le\hbar_f\le-0.15$, $-0.94\le\hbar_\theta\le-0.21$ and $-0.9\le\hbar_\phi\le-0.24$, respectively. Table 2 demonstrates numerical values of convergence at 18^{th}, 21^{st} and 26^{th} iteration. Comparison of results in current study with existing results in literature is done in Tables 3 and 4.

4. Analysis of results

In this section we separately analyze the velocity, temperature and concentration profile of Carreau-Yasuda nanofluid in both shear thinning and thickening cases of blood.

Table 2
Convergence analysis with $We = 0.3$, $\Pr = 1.5$, $d = 0.9$, b, $n = 0.1$, $\beta = 2.2$, $Nt = 0.4$, $Ec = 0.1$, $\sigma = 0.6$, $Nb = 0.4$, $v^* = 0.40$, $Sc = 0.9$, $\delta = 0.6$, $m = 0.4$, $S = 0.5$, $A = 0.1$, $\tilde{A} = 0.77$, $M = 2.6$.

Order of approx.	$-F''(0)$	$-\theta'(0)$	$-\phi'(0)$
1	2.777	1.077	1.794
5	2.542	1.078	2.248
9	2.545	1.071	2.312
11	2.577	1.072	2.316
14	2.552	1.072	2.318
15	2.559	1.073	2.318
16	2.559	1.073	2.318
18	2.559	1.073	2.318
21	2.559	1.073	2.318
23	2.559	1.073	2.318
26	2.559	1.073	2.318

Table 3
Validation of -$F''(0)$ when $d = 2$ and $n = 1$ with existing literature.

A	Khan & Azam [54]	Chamka et al. [55]	Mukhopadhyay & Gorla [56]	Present work
0.2	1.06801	–	–	1.06817
0.4	1.13469	–	–	1.13426
0.8	1.26104	1.261512	1.261479	1.26144
1.2	1.37772	1.378052	1.377850	1.37750
1.4	1.43284	–	–	1.43278
2.0	1.58737	–	–	1.58741

Table 4
Validation of -$\theta''(0)$ when $d = 2$ and $n = 1$ with existing literature.

Pr	Chen [57]	Grubka & Bobba [58]	Sharma [59]	Present work
0.72	1.08853	1.0885	1.0885	1.08845
1.00	1.33334	1.3333	1.3332	1.33361
3.00	2.50972	2.5097	2.5092	2.50992
10.0	4.79686	4.7969	4.7945	4.79685

4.1. Velocity profile

We investigate the behavior of blood velocity against various dimensionless fluid parameters in Figs. 2 and 3. Fig. 2(a) shows dual behavior of velocity profile in case of increasing Weissenberg number. Higher values of We decrease viscous forces between fluid layers that is inverse relation among We and viscosity is developed, hence shear thinning ($n = 0.5$) shows increase in velocity while shear thickening ($n = 1.5$) demonstrates decrease in fluid velocity. In Fig. 2(b) increase in unsteady parameter increases the fluid velocity in case of shear thinning while decrease in velocity in shear thickening. Magnetic interaction parameter shows similar increasing behavior for both thinning and thickening cases (see Fig. 2(c)). The behavior of velocity against stretching parameter A is presented in Figs. 2(d) to 2(f). Since this parameter represents stretching ratios of both of the sheets, so for either sheet stretching more than the other, increase in velocity is seen. But if stretching rates of both sheets are same i.e., $A = 1$, then decrement in velocity is observed for both thinning and thickening cases.
Figs. 3(a) and 3(b) show increasing velocity for increase in both porosity parameter β and fluid parameter n. Fig. 3(c) shows opposite behavior for shear thinning and thickening fluid as fluid parameter d increases. In case of suction and injection, fluid velocity is elevated in Fig. 3(d) for both fluid behaviors.

4.2. Temperature profile

Behavior of fluid temperature against pertinent fluid parameters is depicted in Figs. 4 and 5. Fig. 4(a) demonstrates increasing temperature when Prandtl number increases. Higher Pr results in elevated thermal diffusivity which causes increase in temperature. Eckert number Ec shows different behavior in fluid thickening and thinning cases in Fig. 4(b). Eckert number Ec physically characterizes the self heating property of a fluid. It is the ratio of kinetic energy and enthalpy. At high velocity of fluid (thinning fluid $n = 0.5$) temperature not only changes due to thermal diffusivity but also frictional forces in fluid layers. Hence increase in Ec increases the fluid temperature in case of shear thinning while an opposite behavior is seen in shear thickening ($n = 1.5$). Unsteadiness parameter $\tilde{A}$ shows decrease in temperature profile for both shear thinning and thickening cases, because increasing $\tilde{A}$ results in more heat loss from walls (see Fig. 4(c)). Fig. 4(d) depicts opposite behavior of thinning and thickening fluid against fluid parameter d.

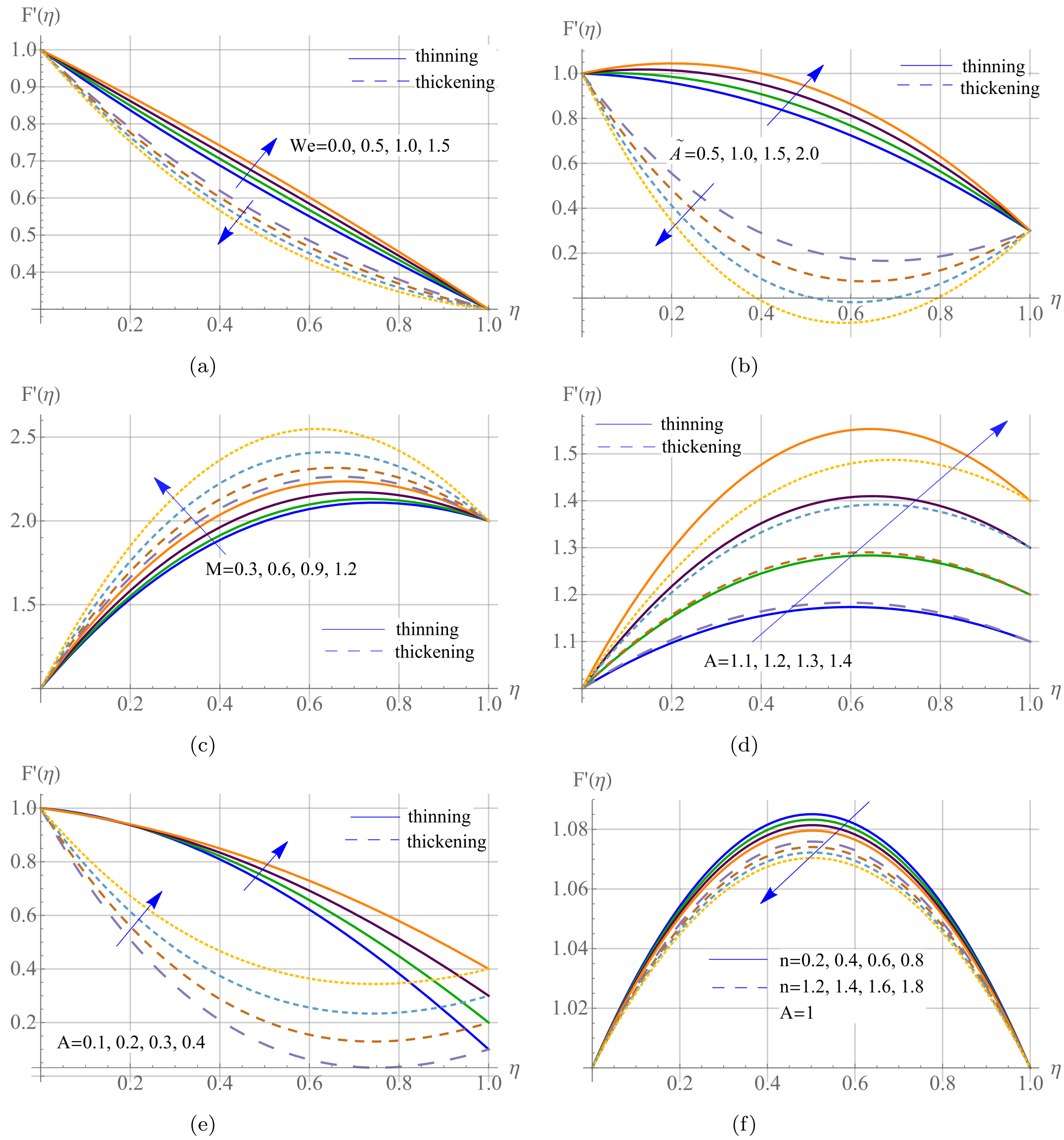

Fig. 2. Effect of We, $\tilde{A}$, M and A on fluid velocity.

Magnetic interaction parameter shows opposite behaviors for both type of temperature in Fig. 5(a). It is seen in shear thinning case that fluid temperature decreases for $\eta < 0.5$ and increases when $\eta > 0.5$. On the other hand, opposite is observed for thickening case. Both Nb and Nt showed increasing temperature profile in either case (thinning or thickening) in Figs. 5(b) and 5(c) which is justified because higher Brownian motion increases random colloidal motion of particles and thermophoresis parameter enhances particle diffusion resulting in fluid temperature elevation. In Fig. 5(d), increase in We shows increasing temperature of the fluid for shear thinning case, and a decreasing temperature for shear thickening case. Weissenberg number gives relation among relaxation of stress and time required for a specific process. Stress relaxation being higher for shear-thinning gives higher temperature whereas in shear thickening, lower stress relaxation yields low temperature.

4.3. Concentration profile

Change in blood concentration against increasing values of various fluid parameters is shown in Figs. 6 and 7. The effect of Brownian motion and thermophoresis parameters on the concentration profile is seen in Figs. 6(a) and 6(b). It is seen that nanoparticle concentration decreases with an increase in Nb whereas Nt shows opposite behavior. Weissenberg number shows decrease in fluid concentration for shear thinning and increase in concentration for thickening cases (see Fig. 6(c)). As We is ratio of elastic forces to viscous forces, so it has inverse relation to viscous property of fluid under study. Hence in case of shear thinning fluid ($n = 0.5$, less viscous forces) increasing We decreases concentration profile while for shear thickening ($n = 1.5$, higher viscous forces) concentration

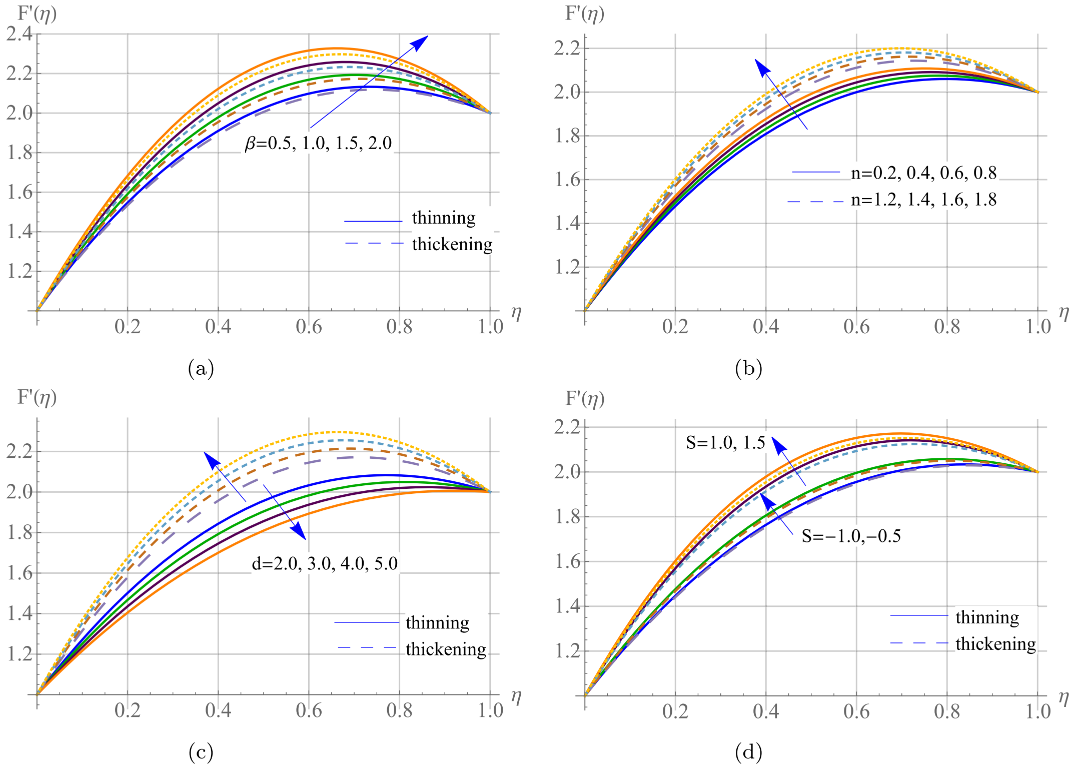

Fig. 3. Effect of β, n, d and S on fluid velocity.

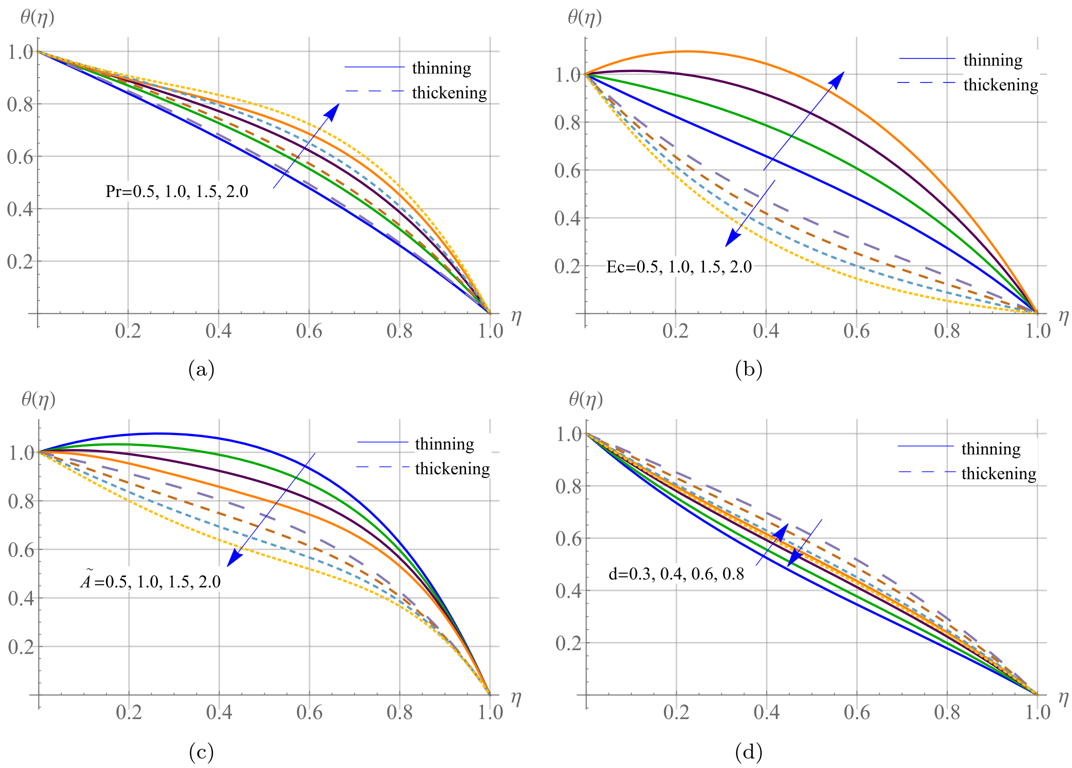

Fig. 4. Effect of Pr, Ec, $\tilde{A}$ and d on fluid temperature.

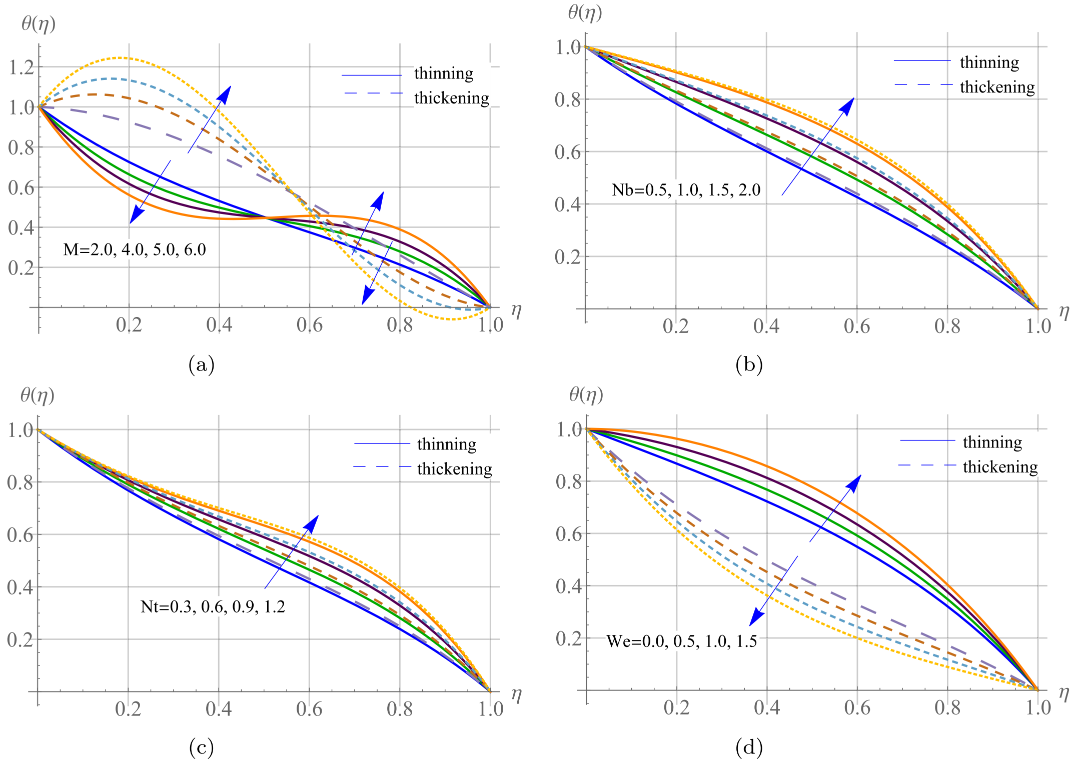

Fig. 5. Effect of M, Nb, Nt and We on fluid temperature.

shows decrement. In Fig. 6(d) rise in unsteadiness parameter depicts increase in fluid concentration. Figs. 6(e) and 6(f) demonstrate decrease in concentration profile against increasing Sc and δ.

The parameter of activation energy $\nu*$ and the chemical reaction σ have opposite effects on concentration profile as seen in Figs. 7(a) and 7(b). Rising activation energy points to increasing E_a motivating more drug flow through blood indicating higher concentration. Elevated E_a and consequently higher temperature results in lower reaction rate showing contrasting behavior of σ on concentration of blood. Mass transfer parameter S and magnetic interaction parameter M decreases fluid concentration for both shear thinning or thickening behavior of fluid (see Figs. 7(c) and 7(d)).

5. Conclusion

In this article, unsteady non-Newtonian fluid has been modeled and solved to depict the results related to blood flow analysis under various circumstances. This investigation provides valuable input for medical analysts seeking effects of chemical reactions and viscous dissipation on drug transport and magnetic therapy treatment of numerous diseases. Homotopy analysis method is used to obtain convergent series solution prior to further fluid analysis. $\hbar$-plots are presented to obtain convergent results. To validate the obtained results, the solutions of this study are also compared with existing results in literature. The focus of current investigation is to show the results related to various fluid parameters on flow regime of Carreau-Yasuda nanofluid for both shear thinning and thickening cases of blood flow. These simulations can be used for predicting blood flow for better diagnosis and treatments in future. Analysis of current results reveals that the magnetic field increases the blood flow in both shear thinning and thickening cases. In shear thinning case, increase in MHD parameter decreases temperature profile when $\eta < 0.5$ and increases when $\eta > 0.5$, on the other hand opposite behavior has been recorded in shear thickening case. Moreover, increase in chemical reaction shows direct relationship with fluid concentration which results in enhanced drug transport through vessels. Increase in Weissenberg number, which determines the orientation of flow, increases blood velocity in shear thinning while decrease has been observed in thickening scenario. It is also noted that Weissenberg number has similar effect (like velocity) on temperature profile while opposite effect on concentration profile. Furthermore, the mass transfer parameter which characterizes the suction/injection phenomena has shown decrease in concentration and hence decreasing drug transport in human body.

Funding statement

This research did not receive any specific grant from funding agencies in the public, commercial, or not-for-profit sectors.

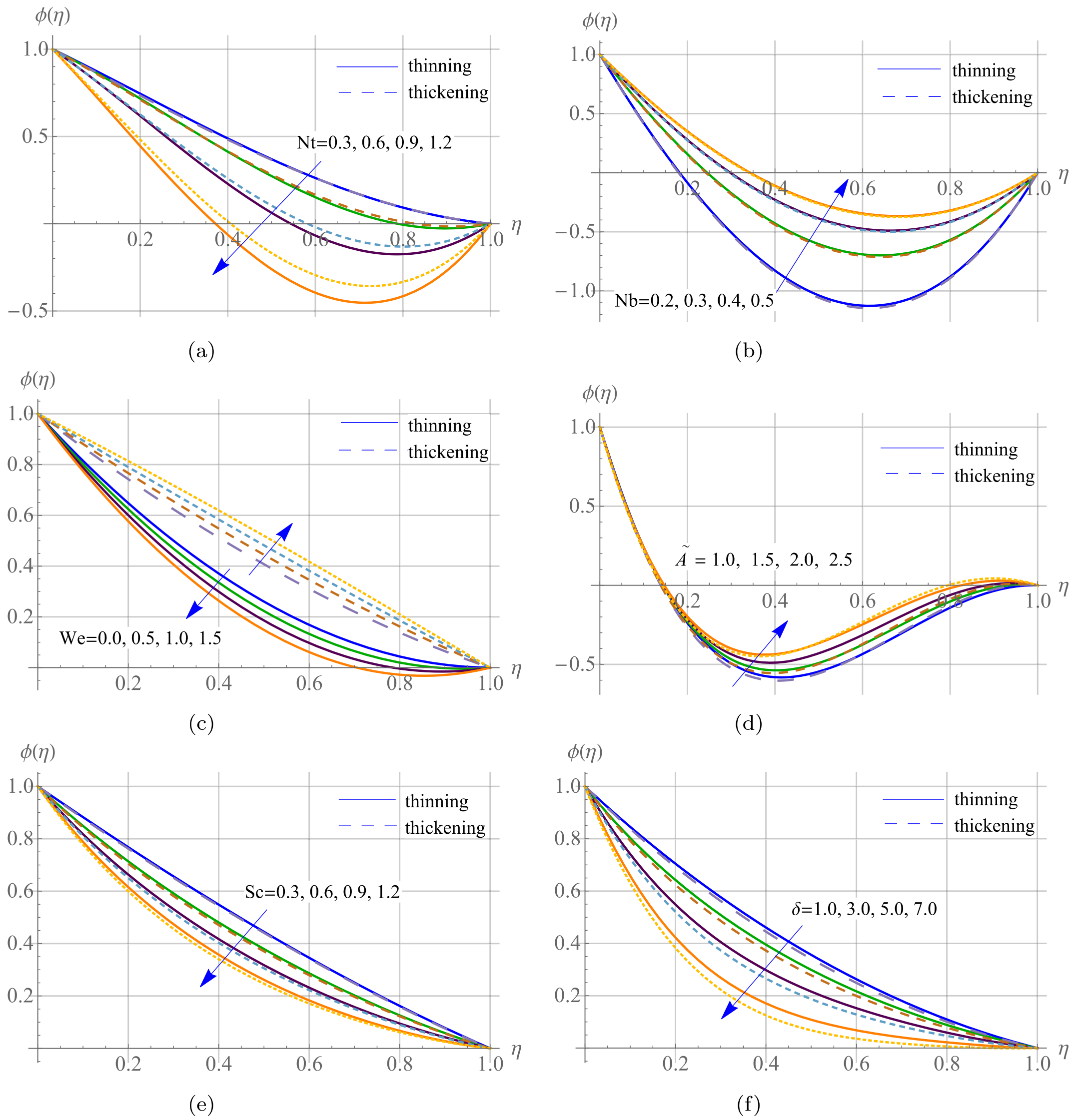

Fig. 6. Effect of Nt, Nb, We, $\tilde{A}$, Sc and δ on fluid concentration.

CRediT authorship contribution statement

Mubashir Qayyum: Conceived and designed the experiments; Analyzed and interpreted the data; Contributed reagents, materials, analysis tools or data; Wrote the paper.

Muhammad Bilal Riaz: Analyzed and interpreted the data; Contributed reagents, materials, analysis tools or data; Wrote the paper.

Sidra Afzal: Performed the experiments; Analyzed and interpreted the data; Wrote the paper.

Declaration of competing interest

The authors declare that they have no known competing financial interests or personal relationships that could have appeared to influence the work reported in this paper.

Data availability

Data included in article/supp. material/referenced in article.

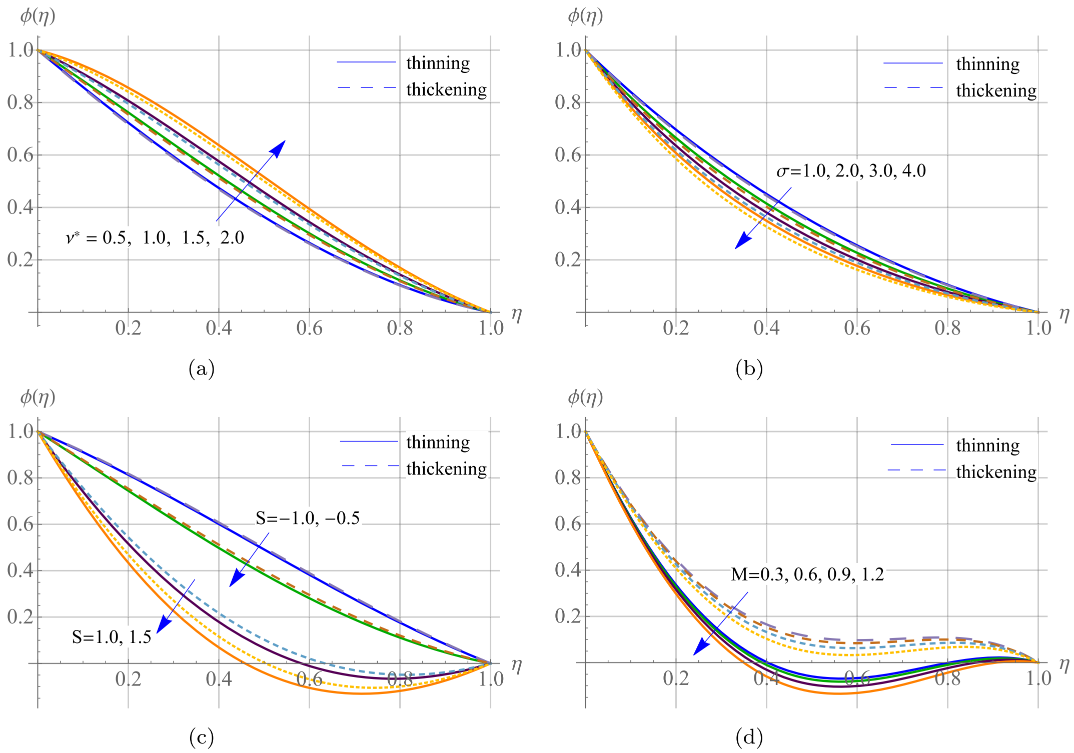

Fig. 7. Effect $\nu*$, σ, S and M on fluid concentration.

References

[1] L. Morris, P. Delassus, A. Callanan, M. Walsh, F. Wallis, P. Grace, T. McGloughlin, 3-D numerical simulation of blood flow through models of the human aorta, J. Biomech. Eng. 127 (2005) 767–775.

[2] M.Y.A. Jamalabadi, M. Daqiqshirazi, H. Nasiri, M.R. Safaei, T.K. Nguyen, Modeling and analysis of biomagnetic blood Carreau fluid flow through a stenosis artery with magnetic heat transfer: a transient study, PLoS ONE 13 (2018) e0192138.

[3] S. Nadeem, M.N. Kiani, A. Saleem, A. Issakhov, Microvascular blood flow with heat transfer in a wavy channel having electroosmotic effects, Electrophoresis 41 (2020) 1198–1205.

[4] A.M. Zidan, L.B. McCash, S. Akhtar, A. Saleem, A. Issakhov, S. Nadeem, Entropy generation for the blood flow in an artery with multiple stenosis having a catheter, Alex. Eng. J. 60 (2021) 5741–5748.

[5] A. Saleem, S. Akhtar, S. Nadeem, Bio-mathematical analysis of electro-osmotically modulated hemodynamic blood flow inside a symmetric and nonsymmetric stenosed artery with joule heating, Int. J. Biomath. 15 (2021).

[6] J. Boyd, J.M. Buick, S. Green, Analysis of the Casson and Carreau-Yasuda non-Newtonian blood models in steady and oscillatory flows using the lattice Boltzmann method, Phys. Fluids 19 (2007) 093103.

[7] A. Shamekhi, K. Sadeghy, Cavity flow simulation of Carreau–Yasuda non-Newtonian fluids using PIM meshfree method, Appl. Math. Model. 33 (2009) 4131–4145.

[8] L.C.F. Andrade, J.A. Petronílio, C.E. de A. Maneschy, D.O. de A. Cruz, The Carreau-Yasuda fluids: a skin friction equation for turbulent flow in pipes and Kolmogorov dissipative scales, J. Braz. Soc. Mech. Sci. 29 (2007) 162–167.

[9] M.B. López, A. Teijeiro, J. Rivas, Magnetic nanoparticle-based hyperthermia for cancer treatment, Rep. Pract. Oncol. Radiother. 18 (2013) 397–400.

[10] S. Rotundo, D. Brizi, A. Monorchio, A feasibility study of a radio-frequency theranostic device for tumor localization and treatment, in: 16th European Conference on Antennas and Propagation (EuCAP), 2022, pp. 1–4.

[11] A.S. Lübbe, C. Alexiou, C. Bergemann, Clinical applications of magnetic drug targeting, J. Surg. Res. 95 (2001) 200–206.

[12] J. Seidl, R. Knuechel, L.A. Kunz-Schughart, Evaluation of membrane physiology following fluorescence activated or magnetic cell separation, Cytometry 36 (1999) 102–111.

[13] E. Morita, N. Ohtsuka, Y. Shindo, S. Nouda, T. Kuramoto, T. Inoue, M. Murano, E. Umegaki, K. Higuchi, In vivo trial of a driving system for a self-propelling capsule endoscope using a magnetic field (with video), Gastroint. Endosc. 72 (2010) 836–840.

[14] A. Kolin, J.H. Grollman Jr., R.J. Steckel, H.D. Snow, Determination of arterial blood flow by percutaneously introduced flow sensors in an external magnetic field, II. Implementation of the method in vivo, Proc. Natl. Acad. Sci. 68 (1971) 29–33.

[15] O. Prakash, S.P. Singh, D. Kumar, Y.K. Dwivedi, A study of effects of heat source on MHD blood flow through bifurcated arteries, AIP Adv. 1 (2011) 042128.

[16] K. Das, G.C. Saha, Arterial MHD pulsatile flow of blood under periodic body acceleration, Bull. Soc. Math. Banja Luka 16 (2009) 21–42.

[17] M.V.S. Rao, K. Gangadhar, P.L.N. Varma, A spectral relaxation method for three-dimensional MHD flow of nanofluid flow over an exponentially stretching sheet due to convective heating: an application to solar energy, Indian J. Phys. 92 (2018) 1577–1588.

[18] A. Tanveer, M. Khan, T. Salahuddin, M.Y. Malik, F. Khan, Theoretical investigation of peristaltic activity in MHD based blood flow of non-Newtonian material, Comput. Methods Programs Biomed. 187 (2020) 105225.

[19] M.M. Bhatti, M.M. Rashidi, Study of heat and mass transfer with Joule heating on magnetohydrodynamic (MHD) peristaltic blood flow under the influence of Hall effect, Propuls. Power Res. 6 (2017) 177–185.

[20] K.V. Ramana, K. Gangadhar, T. Kannan, et al., Cattaneo–Christov heat flux theory on transverse MHD Oldroyd-B liquid over nonlinear stretched flow, J. Therm. Anal. Calorim. 147 (2022) 2749–2759.
[21] K. Elangovan, K. Subbarao, K. Gangadhar, An analytical solution for radioactive MHD flow TiO2–Fe3O4/H2O nanofluid and its biological applications, Int. J. Ambient Energy 43 (2022) 7576–7587.
[22] K. Gangadhar, T. Kannan, P. Jayalakshmi, Magnetohydrodynamic micropolar nanofluid past a permeable stretching/shrinking sheet with Newtonian heating, J. Braz. Soc. Mech. Sci. Eng. 39 (2017) 4379–4391;
A.J. Chamka, On laminar hydromagnetic mixed convection flow in a vertical channel with symmetric and asymmetric wall heating conditions, Int. J. Eng. Sci. 45 (2002) 2509–2525.
[23] K. Gangadhar, D.N. Bhargavi, M.R.S. Venkata, A.J. Chamkha, Entropy minimization on magnetized Boussinesq couple stress fluid with non-uniform heat generation, Phys. Scr. 96 (2021) 095205.
[24] F. Selimefendigil, H.F. Öztop, A.J. Chamkha, Role of magnetic field on forced convection of nanofluid in a branching channel, Int. J. Numer. Methods Heat Fluid Flow 30 (2020) 1755–1772.
[25] N. Saleem, S. Munawar, D. Tripathi, Thermal analysis of double diffusive electrokinetic thermally radiated TiO2-Ag/blood stream triggered by synthetic cilia under buoyancy forces and activation energy, Phys. Scr. 96 (2021) 095218.
[26] K. Gangadhar, E.M. Victoria, K.B. Lakshmi, A.J. Chamkha, Nonlinear radiation phenomena for Casson–Maxwell nanoliquid flow with chemical reactions, Proc. Inst. Mech. Eng., E J. Process Mech. Eng. (2022).
[27] M. Ramzan, A. Rafiq, J.D. Chung, S. Kadry, Y.-M. Chu, Nanofluid flow with autocatalytic chemical reaction over a curved surface with nonlinear thermal radiation and slip condition, Sci. Rep. 10 (2020) 18339.
[28] L.B. McCash, I. Zehra, A. Al-Zubaidi, M. Amjad, N. Abbas, S. Nadeem, Combined effects of binary chemical reaction/activation energy on the flow of Sisko fluid over a curved surface, Crystals 11 (2021) 967.
[29] B. Yu, M. Ramzan, S. Riasat, M. Kadry, Y.-M. Chu, M.Y. Malik, Impact of autocatalytic chemical reaction in an Ostwald-de-Waele nanofluid flow past a rotating disk with heterogeneous catalysis, Sci. Rep. 11 (2021) 15526.
[30] M.I. Khan, F. Alzahrani, Activation energy and binary chemical reaction effect in nonlinear thermal radiative stagnation point flow of Walter-B nanofluid: numerical computations, Int. J. Mod. Phys. B 34 (2020) 2050132.
[31] R.J. Punith Gowda, R. Naveen Kumar, A.M. Jyothi, B.C. Prasannakumara, I.E. Sarris, Impact of binary chemical reaction and activation energy on heat and mass transfer of Marangoni driven boundary layer flow of a non-Newtonian nanofluid, Processes 9 (2021) 702.
[32] K. Gangadhar, K.B. Lakshmi, T. Kannan, A.J. Chamkha, Stefan blowing on chemically reactive nano-fluid flow containing gyrotactic microorganisms with leading edge accretion (or) ablation and thermal radiation, Indian J. Phys. 96 (2022) 2827–2840.
[33] T. Hayat, S.A. Khan, A. Alsaedi, H.M. Fardoun, Marangoni forced convective flow of second grade fluid with irreversibility analysis and chemical reaction, Int. J. Thermophys. 42 (2021) 1–21.
[34] I. Ullah, T. Hayat, A. Alsaedi, S. Asghar, Modeling for radiated Marangoni convection flow of magneto-nanoliquid subject to activation energy and chemical reaction, Sci. Iran. 27 (2020) 3390–3398.
[35] B. Shankar Goud, M.M. Nandeppanavar, Ohmic heating and chemical reaction effect on MHD flow of micropolar fluid past a stretching surface, Partial Differ. Equ. Appl. Math. 4 (2021) 100104.
[36] T.H. Zhao, M.I. Khan, Y.M. Chu, Artificial neural networking (ANN) analysis for heat and entropy generation in flow of non-Newtonian fluid between two rotating disks, Math. Methods Appl. Sci. (2021) 1–19.
[37] R. Gandhi, B.K. Sharma, C. Kumawat, O.A. Bég, Modeling and analysis of magnetic hybrid nanoparticle (Au-Al2O3/blood) based drug delivery through a bell-shaped occluded artery with joule heating, viscous dissipation and variable viscosity effects, Proc. Inst. Mech. Eng., E J. Process Mech. Eng. (2022) 095440892210802.
[38] D. Yang, M. Yasir, A. Hamid, Thermal transport analysis in stagnation-point flow of Casson nanofluid over a shrinking surface with viscous dissipation, Waves Random Complex Media (2021) 1–15.
[39] A.M. Megahed, M.G. Reddy, Numerical treatment for MHD viscoelastic fluid flow with variable fluid properties and viscous dissipation, Indian J. Phys. 95 (2020) 673–679.
[40] Y.M. Chu, U. Khan, A. Zaib, S.H.A.M. Shah, Numerical and computer simulations of cross-flow in the streamwise direction through a moving surface comprising the significant impacts of viscous dissipation and magnetic fields: stability analysis and dual solutions, Math. Probl. Eng. (2020) 8542396.
[41] H. Wang, Y. Su, R. Qiao, J. Wang, W. Wang, Investigate effects of microstructures on nanoconfined water flow behaviors from viscous dissipation perspectives, Transp. Porous Media 140 (2021) 815–836.
[42] F. Mabood, A. Mastroberardino, Melting heat transfer on MHD convective flow of a nanofluid over a stretching sheet with viscous dissipation and second order slip, J. Taiwan Inst. Chem. Eng. 57 (2015) 62–68.
[43] M.S. Hashmi, N. Khan, S.U. Khan, M.I. Khan, N.B. Khan, M. Nazeer, S. Kadry, Y.M. Chu, Dynamics of coupled reacted flow of Oldroyd-B material induced by isothermal/exothermal stretched disks with Joule heating, viscous dissipation and magnetic dipoles, Alex. Eng. J. (2020).
[44] M.I. Khan, S. Afzal, T. Hayat, M. Waqas, A. Alsaedi, Activation energy for the Carreau-Yasuda nanomaterial flow: analysis of the entropy generation over a porous medium, J. Mol. Liq. 297 (2020) 111905.
[45] A. Bhattacharyya, G.S. Seth, R. Kumar, A.J. Chamka, Simulation of Cattaneo–Christov heat flux on the flow of single and multi-walled carbon nanotubes between two stretchable coaxial rotating disks, J. Therm. Anal. Calorim. 139 (2020) 1655–1670.
[46] A.S. Dogonchi, M.K. Nayak, N. Karimi, A.J. Chamka, D.D. Ganji, Numerical simulation of hydrothermal features of Cu–H2O nanofluid natural convection within a porous annulus considering diverse configurations of heater, J. Therm. Anal. Calorim. 141 (2020) 2109–2125.
[47] D. Toghraie, R. Mashayekhi, H. Arasteh, S. Sheykhi, M. Niknejadi, A.J. Chamkha, Two-phase investigation of water-Al2O3 nanofluid in a micro concentric annulus under non-uniform heat flux boundary conditions, Int. J. Numer. Methods Heat Fluid Flow 30 (2020) 1795–1814.
[48] J.C. Umavathi, A.J. Chamkha, A. Mateen, A. Al-Mudhaf, Unsteady two-fluid flow and heat transfer in a horizontal channel, Heat Mass Transf. 42 (2005) 81–90.
[49] F. Mabood, M. Shamshuddin, S.R. Mishra, Characteristics of thermophoresis and Brownian motion on radiative reactive micropolar fluid flow towards continuously moving flat plate: HAM solution, Math. Comput. Simul. 191 (2022) 187–202.
[50] T. Salahuddin, A. Javed, M. Khan, M. Awais, B. Al Alwan, A significant impact of Carreau Yasuda material near a zero velocity region, Arab. J. Chem. 15 (2022) 104166.
[51] M.I. Khana, F. Alzahranib, A.H.Z. Ali, Estimation of entropy generation in Carreau-Yasuda fluid flow using chemical reaction with activation energy, J. Mater. Res. Technol. 9 (2020) 9951–9964.
[52] U. Nazir, M. Sohail, M.M. Selim, H. Alrabaiah, P. Kumam, Finite element simulations of hybrid nano-Carreau Yasuda fluid with hall and ion slip forces over rotating heated porous cone, Sci. Rep. 11 (2021) 19604.
[53] A.J. Chamka, Non-Darcy fully developed mixed convection in porous medium channel with heat generation/absorption and hydromagnetic effects, Numer. Heat Transf., Part A, Appl. 32 (1997) 653–675.
[54] M. Khan, M. Azam, Unsteady heat and mass transfer mechanisms in MHD Carreau nanofluid flow, J. Mol. Liq. 225 (2017) 554–562.
[55] A.J. Chamkha, A.M. Aly, M.A. Mansour, Similarity solution for unsteady heat and mass transfer from a stretching surface embedded in a porous medium with suction/injection and chemical reaction effects, Chem. Eng. Commun. 197 (2010) 846–858.
[56] S. Mukhopadhyay, R.S.R. Gorla, Unsteady MHD boundary layer flow of an upper convected maxwell fluid past a stretching sheet with first order constructive/destructive chemical reaction, J. Naval Archit. Mar. Eng. 9 (2012) 123–133.

[57] C.H. Chen, Laminar mixed convection adjacent to vertical continuously stretching sheets, Heat Mass Transf. 33 (1998) 471–476.
[58] L.J. Grubka, K.M. Bobba, Heat transfer characteristics of a continuous stretching surface with variable temperature, J. Heat Transf. 107 (1985) 248–250.
[59] R. Sharma, Effect of viscous dissipation and heat source on unsteady boundary layer flow and heat transfer past a stretching surface embedded in a porous medium using element free Galerkin method, Appl. Math. Comput. 219 (2012) 976–987.